



# Collagen deposition in the liver is strongly and positively associated with T1rho elongation while fat deposition is associated with T1rho shortening: an experimental study of methionine and choline-deficient (MCD) diet rat model

Feng Zhao<sup>1^</sup>, Nan Zhou<sup>2</sup>, Ji-Li Wang<sup>3</sup>, Hua Zhou<sup>4</sup>, Li-Qiu Zou<sup>5</sup>, Wei-Xiang Zhong<sup>3</sup>, Jian He<sup>2</sup>, Cun-Jing Zheng<sup>6</sup>, Sen-Xiang Yan<sup>1</sup>, Yi Xiáng J. Wáng<sup>6^</sup>

<sup>1</sup>Department of Radiation Oncology, The First Affiliated Hospital, Zhejiang University School of Medicine, Hangzhou, China; <sup>2</sup>Department of Radiology, The Affiliated Drum Tower Hospital of Nanjing University Medical School, Nanjing, China; <sup>3</sup>Department of Pathology, The First Affiliated Hospital, Zhejiang University School of Medicine, Hangzhou, China; <sup>4</sup>Department of Radiology, The First Affiliated Hospital, Zhejiang University School of Medicine, Hangzhou, China; <sup>5</sup>Department of Radiology, The Sixth Affiliated Hospital of Shenzhen University, Shenzhen, China; <sup>6</sup>Department of Imaging and Interventional Radiology, Faculty of Medicine, The Chinese University of Hong Kong, Shatin, Hong Kong SAR, China

*Correspondence to:* Dr. Feng Zhao. Department of Radiation Oncology, the First Affiliated Hospital, Zhejiang University School of Medicine, Hangzhou 310003, China. Email: zju\_zhaofeng@zju.edu.cn; Dr. Yi Xiáng J. Wáng. Department of Imaging and Interventional Radiology, Faculty of Medicine, The Chinese University of Hong Kong, Shatin, Hong Kong SAR, China. Email: yixiang\_wang@cuhk.edu.hk.

**Background:** A number of questions concerning the histological mechanism of elongated T1rho in liver fibrosis remain unanswered. Using a rat model of non-alcoholic fatty liver disease (NAFLD) induced with methionine and choline-deficient (MCD) diet, the primary aim of this study is to clarify whether collagen deposition *per se* causes liver T1rho elongation.

**Methods:** There were 45 rats in the NAFLD model group and 8 rats in the control group. NAFLD model rats were fed MCD diet for 1, 2, 4, 6, 8, or 10 weeks, respectively. At the endpoint, the rats had *in vivo* MRI at 3.0 T and followed by histology. For T1rho data acquisition, a rotary echo spin-lock pulse was implemented in a three-dimensional fast field echo sequence with frequency selective fat suppression. The spin-lock frequency was set to 500 Hz, and the spin-lock times of 5, 10, 40, and 50 ms were used. Liver specimens were processed with hematoxylin-eosin staining for steatosis and inflammation evaluation, and Masson's trichrome staining for collagen visualization. The semiquantitative histopathological evaluation was based on NASH Clinical Research Network criteria. Histomorphometric analysis calculated percentages of fat and collagen accumulations in the livers.

**Results:** A strong ( $r=0.82$ ) and significant ( $P<0.0001$ ) positive correlation between liver collagen content and liver T1rho was observed. Rats with no or minimal inflammation could have very long T1rho value. Among experimental rats without a positive fibrosis grading, five rats did not have an inflammation score (i.e., had minimal inflammation or no inflammation) while four had a positive inflammation score; the difference in liver T1rho between these two types of rats was minimal. Eight control rat livers and 15 stage-1 fibrosis rat livers were separated by liver T1rho completely. When four subgroups of experiment rats were selected where the liver collagen had a very narrow range within these subgroups, all these four subgroups showed a trend of negative correlation between liver fat and liver T1rho.

**Conclusions:** Collagen deposition in the live strongly contributes to liver T1rho elongation, while fat deposition contributes to T1rho shortening. In a well-controlled experimental setting, T1rho measure alone allows separation of healthy livers and stage-1 liver fibrosis in the MCD rat liver model.

<sup>^</sup> ORCID: Feng Zhao, 0000-0002-4441-9992; Yi Xiáng J. Wáng, 0000-0001-5697-0717.

**Keywords:** T1rho; liver fibrosis; liver steatosis; collagen; non-alcoholic fatty liver disease (NAFLD)

Submitted May 12, 2020. Accepted for publication Sep 22, 2020.

doi: 10.21037/qims-20-651

View this article at: <http://dx.doi.org/10.21037/qims-20-651>

## Introduction

Liver fibrosis, a common feature of almost all chronic liver diseases, involves the accumulation of collagen, proteoglycans, and other macromolecules in the extracellular matrix. Clinically liver fibrosis usually has an insidious onset and progresses slowly over decades. To date, noninvasive diagnostic tests available from clinical practice are not sensitive or specific enough to detect occult liver injury at early stages. Liver biopsy is currently the standard of reference for the diagnosis and staging of liver fibrosis. However, it is an invasive procedure with possible complications. Histologic assessment of fibrosis is also an inherently subjective process, and subject to sampling variability. A noninvasive and quantitative technique for assessing liver fibrosis and monitoring disease progression or therapeutic intervention is highly desirable.

T1rho (T1 $\rho$ ) relaxation time describes spin-lattice relaxation in the rotation frame at the presence of an external radiofrequency pulse in the transverse plane. Numerous pre-clinical studies reported the potential usefulness of T1rho MR imaging for assessment liver fibrosis, with the elongation of T1rho value correlated severity of fibrosis (1-6). A number of clinical studies in human subjects have also been reported (7-17). In a group of 25 healthy volunteers and 35 cirrhosis patients, Allkemper *et al.* (9) reported that T1rho value was significantly associated with the Child-Pugh staging of the patients. In patients with chronic liver diseases, Takayama *et al.* (11) demonstrated liver T1rho values showed significant positive correlations with the serum levels of total bilirubin, direct bilirubin, and indocyanine green (ICG-R15), and significant negative correlations with the serum levels of albumin and  $\gamma$ -glutamyl transpeptidase. Recently, more reports confirmed diseased livers have longer T1rho measure than healthy livers, and elongated liver T1rho is associated comprised liver function (13-17).

Despite these publications, a number of questions concerning the histological mechanism of elongated T1rho in liver fibrosis remain unanswered (18,19). Liver 'fibrosis process', depending on its causes, is associated with a number of complicated pathological processes, including

steatosis, hepatocellular ballooning, inflammation, as well as collagen deposition. Inflammation involves presence of inflammatory cells, including lymphocytes, eosinophils and neutrophils, near ballooned hepatocytes. Researchers in prior studies have observed T1rho elongation in conditions associated with depletion of macromolecules (20), but liver 'fibrosis process' is associated with macromolecular accumulation (collagen deposition) rather than depletion. Though it has been reported the higher extent of liver collagen deposition is seen with longer liver T1rho measure, it has been hypothesized that the primary contributor to liver T1rho elongation in 'fibrosis process' might be the inflammation rather than collagen deposition (6,18,19). Using a rat model of liver fibrosis induced with the methionine and choline-deficient (MCD) diet, the primary aim of this study is to clarify whether collagen deposition *per se* causes liver T1rho elongation. Compared with the commonly used CCl<sub>4</sub> intoxication model and biliary duct ligation (BDL) model, the diet induced model has the advantage that it is pathophysiologically more similar to the non-alcoholic fatty liver disease (NAFLD) and non-alcoholic steatohepatitis (NASH) process in human patients.

## Methods

### Animals

This study was approved by the local Animal Experimentation Ethics Committee (NO. 2017-217), and conducted in compliance with institutional guidelines for the care and use of animals of Zhejiang University School of Medicine and Nanjing University Medical School, China. Fifty-eight 8-week old male Sprague-Dawley rats with initial weights between 250 and 300 g were used. The animals were housed on a 12-h light/12-h dark cycle in an airconditioned room at 25 °C. Food and water were available ad libitum. Bodyweight was recorded daily.

Rats were divided into two groups randomly, with 50 rats in the NAFLD model group and 8 in the control group. After one week of acclimatization with control diet (A02082003B, Research Diets Inc., USA), NAFLD model group rats were fed MCD diet (A02082002B,

Research Diets Inc., USA) with 1, 2, 4, 6, 8, or 10 weeks, respectively. Five rats in the NAFLD model group died during anesthesia for MRI. Finally, 45 NAFLD model rats (week-1, n=4; week-2, n=9; week-4, n=8; week-6, n=8; week-8, n=8; week-10, n=8) were available for final analysis, with end-stage *in vivo* MRI and followed by histology. The 8 control rats had MRI and then histology after one week of acclimatization with control diet.

### MR imaging and image analysis

MRI was performed in Nanjing, China, on a 3.0T MR scanner (Ingenia; Philips Medical Systems, Best, the Netherlands), using a 16-channel human head & neck phased array coil. The T1rho sequence was provided via Academic Medical Center Amsterdam, the Netherlands. T1rho MRI was performed after anatomical imaging for the liver. For T1rho data acquisition, a rotary echo spin-lock pulse was implemented in a three-dimensional (3D) fast field echo sequence with frequency selective fat suppression. The spin-lock frequency was set at 500Hz, and the spin-lock times (TSL) of 5, 10, 40, and 50 ms (milliseconds) were used. The delay time after each shot acquisition was set to 5,000 ms to restore equilibrium magnetization before the next T1rho preparation. Twelve axial slices were selected to cover the whole liver. TR/TE (ms) =8.0/4.1, FOV=120×120×24 mm<sup>3</sup>; voxel size = 0.61×0.60×2.00 mm<sup>3</sup>, matrix = 200×196, Flip angle =15°, TFE factor =210, number of signal averaging =2. The acquisition duration for MRI-T1rho was 6 minutes 41 seconds.

For magnetic resonance imaging derived proton density fat fraction (MRI-PDFF) measure, mDIXON Quant imaging was obtained by using a 3D fast field echo (FFE) sequence, whose parameters were as follows: TR =12 ms, TE1 =1.45 ms, delta TE=1.2 ms with 6 echoes acquired. Twelve axial slices were scanned to cover the whole liver. FOV=100×100×24 mm<sup>3</sup>; voxel size=1.2×1.2×2 mm<sup>3</sup>; number of signal averaging =16. A low flip angle of only 3 degrees was applied to limit the T1 bias. The acquisition duration was 2 minutes 48 seconds.

T1rho maps were computed on a pixel-by-pixel basis using mono-exponential decay {Eq. [1]} model with an in-house developed MATLAB program (Mathworks, Natick, MA, USA):

$$M(TSL) = M0 \cdot \exp(-TSL/T1rho) \quad [1]$$

Where M0 and M (TSL) denote the equilibrium magnetization and T1rho-prepared magnetization with the spin-lock time of TSL, respectively. In order to avoid the

influence of gas from the lungs and gastrointestinal tract on the scanning images, the upper and lower 2 slices images were excluded for analysis. Therefore, the only 8 slices were included for T1rho mapping and measurements. T1rho value measurement method was regions-of-interest (ROIs) methods as same as our former study reported, which is setting 5 ROIs in each slice with avoiding blood vessels and artifacts (1,2) (Figure 1).

Quantitative PDFF maps were calculated after the acquisition of mDIXON Quant sequence. The same as T1rho measurement, the central 8 slices images were measured with ROI based approach using RadiAnt DICOM Viewer (version 5.5.0; <https://www.radiantviewer.com/>).

### Histopathological examination

For histologic examination, animals were sacrificed within 4 hours after MRI. Liver specimens were fixed in 4% phosphate-buffered formaldehyde and embedded in paraffin. Sections of 5 μm thick were dewaxed in xylene and rehydrated in a series of ethanol. Hematoxylin-eosin (H & E) staining was processed for steatosis and inflammation evaluation. Masson's trichrome staining was applied for collagen visualization. Histology was assessed independently by a liver histopathologist (WX. Z., with 15-year experience).

The quantitative histopathological evaluation of steatosis and fibrosis was analyzed by histomorphometric analysis with a computerized image analysis system comprised of a photomicroscope and digital camera (Olympus; KF-PRO-020 Digital slice scanner, Ningbo, China) and software (K-Viewer, version 1.5.2.5, KFBIO Co., Ningbo, China; <http://www.kfbio.cn>). Liver sections stained with H & E staining were assessed for the presence of fat accumulation in 10 systematically sampled areas per section. Then the percentages of fat accumulation (% area) were calculated for each rat. Similarly, liver sections stained with Masson's trichrome staining were assessed for the presence of collagen deposition in 10 systematically sampled areas per section. Then the collagen fractions (% area) were calculated for each rat.

The semiquantitative histopathological evaluation was based on NASH Clinical Research Network (NASH CRN) criteria including: lobular inflammation score (overall assessment of all inflammatory foci: 0 was no foci, 1 was <2 foci/200× field, 2 was 2–4 foci/200× field, and 3 was >4 foci/200× field), fibrosis stage (0 was no fibrosis, 1 was portal or perisinusoidal fibrosis, 2 was periportal

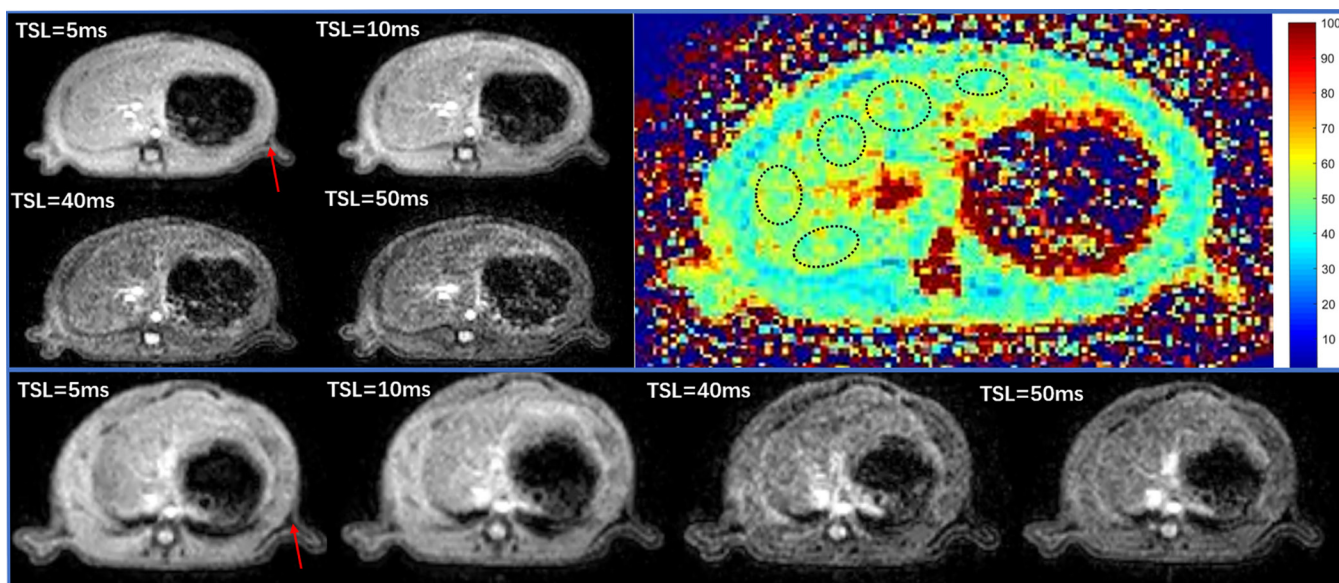


**Figure 1** T1rho images of two rats with T1rho mapping of one of the rats. TSL, spin-lock time. Arrows indicate satisfactory suppression of subcutaneous fat signal. Circles on T1rho map denote region of interests for T1rho measurement.

and perisinusoidal fibrosis, 3 was bridging fibrosis, and 4 was cirrhosis) and steatosis scoring: (evaluation of liver parenchymal involvement by steatosis: 0 is <5%, 1 is 5–33%, 2 is >33–66%, and 3 is >66%) (21) (Figure 2).

### Statistical analysis

Because rat's intakes of MCD diet could not be well-controlled, the rats in the group with the same duration of MCD diet feeding presented different histopathological results. Therefore, the rats in this study were grouped for analysis according to the histological evaluation for liver steatosis scoring, steatotic inflammation scoring and fibrosis staging, rather than the duration of MCD diet feeding.

Data are presented as mean  $\pm$  standard deviation. All statistical analyses were done using SPSS 25.0 (IBM SPSS Statistics, IBM Corporation, Chicago, IL). The Mann-Whitney U test was used for non-paired comparison. A P value <0.05 was considered statistically significant. Strength of correlation was evaluated by using the Pearson correlation coefficient ( $r$ ), with a  $r$  lower than 0.3, indicating weak, 0.3–0.7 indicating moderate; and higher than 0.7 indicating strong correlation.

## Results

Among the total 45 experimental rats, 18, and 27 had

steatosis score of 1, and 2 respectively; 14, 4, and 2 had inflammation score of 1, 2, 3 respectively, 15, 15, and 6 had fibrosis stage of 1, 2, 3 respectively (Table 1). The correlations between collagen content and liver T1rho in 8 control rats and experimental 5 rats with histological diagnosis of no positive inflammation scoring (i.e., with no or minimal inflammation) and no positive fibrosis grading are shown in Figure 3. The results show collagen content was positively associated with T1rho measure even the collagen content was low.

For the experimental rats (total  $n=45$ ), a strong ( $r=0.82$ ) and significant ( $P<0.001$ ) positive correlation between liver collagen content and liver T1rho was observed, with 1% collagen area increase contributed to T1rho value increase of 1.35 ms (Figure 4A). There was a weak trend that higher liver inflammation was associated with longer liver T1rho measure (Figure 2B,  $r=0.25$ ,  $P=0.1$ ). However, it can be noted that a number of rats with no or minimal inflammation had very long T1rho value (Figure 4B).

Despite not graded as having developed fibrosis, 9 experimental rats in Figure 5 differ from control rats that they had increased liver collagen, this was translated to longer liver T1rho. Among experimental rats without fibrosis grading, five rats did not have positive inflammation score (i.e., minimal inflammation or no inflammation) while four had positive inflammation score. The difference in liver T1rho between these two types of rats were minimal.

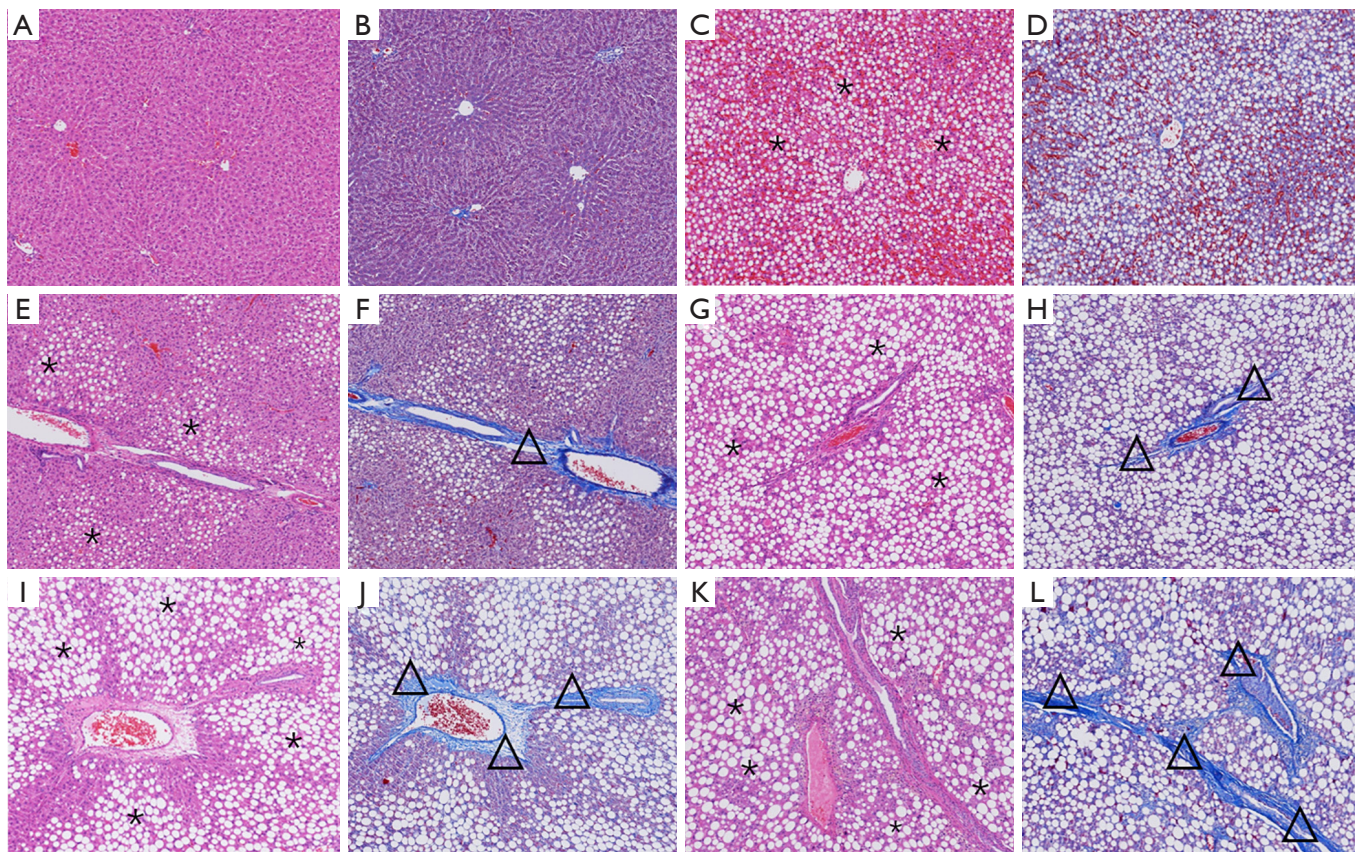


**Figure 2** H & E staining (A,C,E,G,I,K) and Masson's trichrome staining (B,D,F,H,J,L) of liver in different rats with representative stages of liver fatty and fibrosis (original magnification, ×100). (A,B) Steatosis grade 0, Fibrosis stage 0; (C,D) Steatosis grade 1, Fibrosis stage 0; (E,F) Steatosis grade 1, Fibrosis stage 2; (G,H) Steatosis grade 2, Fibrosis stage 1; (I,J) Steatosis grade 2, Fibrosis stage 2; (K,L) Steatosis grade 2, Fibrosis stage 3. \*, fat accumulation, Δ, collagen deposition.

**Table 1** The relationship between methionine and choline-deficient (MCD) diet feeding duration and the development of liver inflammation and fibrosis in experimental rats

MCD diet feeding duration	Steatosis scoring				Inflammation scoring				Fibrosis grading			
	S0	S1	S2	S3	I0	I1	I2	I3	F0	F1	F2	F3
1 week		4			3	1			4			
2 weeks		9			3	3	2	1	5	4		
4 weeks		3	5		7	1				5	3	
6 weeks			8		6	2				4	4	
8 weeks		2	6		4	4				2	2	4
10 weeks			8		2	3	2	1			6	2
Total	0	18	27	0	25	14	4	2	9	15	15	6

S0, S1, S2, S3: steatosis of 0, 1, 2, 3 respectively. I0, I1, I2, I3: inflammation score of 0, 1, 2, 3 respectively. Inflammation score of 0 denotes no or minimal inflammation. F0, F1, F2, F3: fibrosis score of 0, 1, 2, 3 respectively.

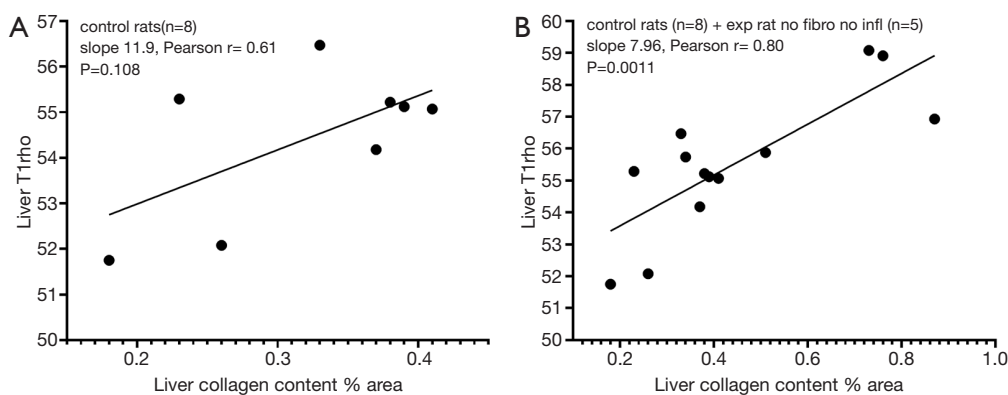


**Figure 3** The correlation between collagen content and liver T1rho (in milliseconds) for rats without pathologic fibrosis. (A) Control rats show a positive trend of higher liver collagen area (percentage measured by histology) correlated longer liver T1rho measure ( $r=0.61$ ,  $P=0.11$ ); (B) in addition to the data in (A), 5 rats from the experiment group are added in the graph. These 5 rats were graded histologically as without positive inflammation score and without positive fibrosis grading. The correlation between collagen area and liver T1rho become statistically significant in B ( $r=0.80$ ,  $P=0.0011$ ).

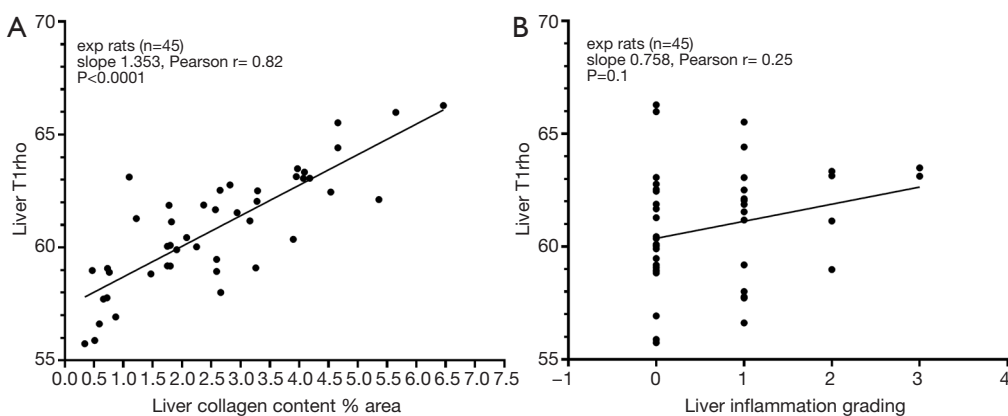


**Figure 4** Correlation between liver T1rho (in milliseconds) and liver collagen content (percentage area measured by histology) or liver inflammation severity. (A) There is a strong and significant positive correlation between liver collagen content and liver T1rho; (B) the correlation between liver T1rho measure and liver inflammation is less strong ( $r=0.25$ ) and not significant ( $P=0.1$ ).

While higher collagen content was associated with longer T1rho measure, the impact on T1rho from inflammation was less notable (Figure 5B).

Rats with positive fibrosis grading had substantially longer T1rho values than those rats without positive fibrosis grading (Figure 6). For the rats with positive fibrosis grading, the rats with positive inflammation scoring had slightly higher liver collagen deposition ( $3.28\% \pm 1.22\%$  vs.  $2.89\% \pm 1.40\%$ ) and also slightly longer liver T1rho ( $62.23 \pm 1.84$  vs.  $61.21 \pm 2.21$  ms) than those without positive inflammation scoring.

The 8 control rat livers and 15 stage-1 fibrosis rat livers were

separately by liver T1rho completely (Figure 7). The longest value of control rat livers was 56.6 ms ( $54.40 \pm 1.65$  ms), while the shortest value of fibrotic rat liver was 58.0 ms. Higher fibrosis grading was associated with longer T1rho value, with stage-1, stage-2, stage-3 liver fibrosis had  $60.01 \pm 1.34$ ,  $62.07 \pm 0.91$ , and  $64.79 \pm 1.34$  ms, respectively (compared with each other, all  $P < 0.01$ ).

The fat percentage quantified by histology and by MRI-PDFP had a very good agreement (Figure 8A). The fat percentage quantified by MRI also had a very good agreement with subjective scoring (Figure 8B). Higher fat content in the liver was significantly and positively correlated

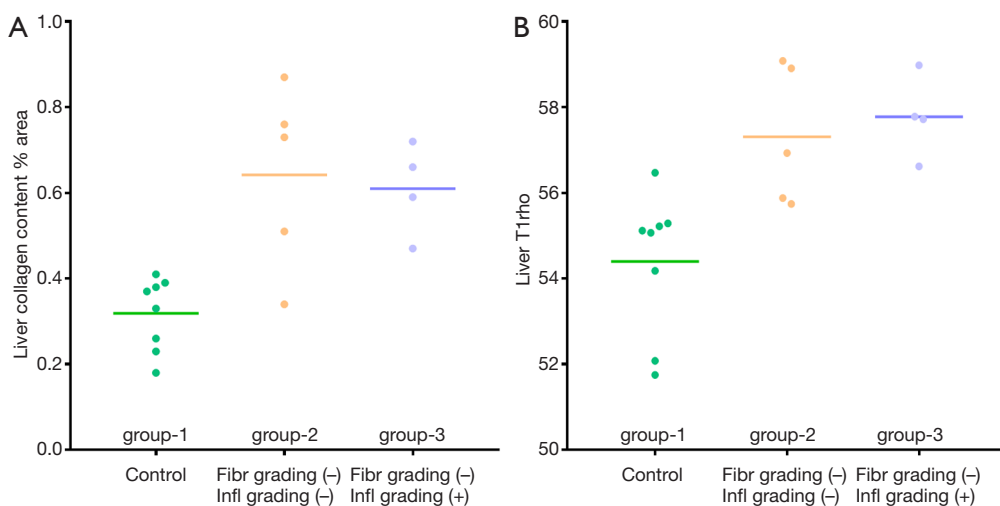


**Figure 5** Liver T1rho measure (in milliseconds) difference between control rats and experimental rats without fibrosis. (A) Liver collagen content (measured in percentage area by histology) among three types of rats. (B) Liver T1rho among three types of rats. Group-1 are control rats. Both group-2 and group-3 are experimental rats without positive fibrosis grading [fibr grading (-)]. Group-2 had no or minimal inflammation [infl grading (-)]. Group-3 had positive inflammation scoring [infl grading (+)], with three rats of inflammation score-1 and one rat of inflammation score-2.

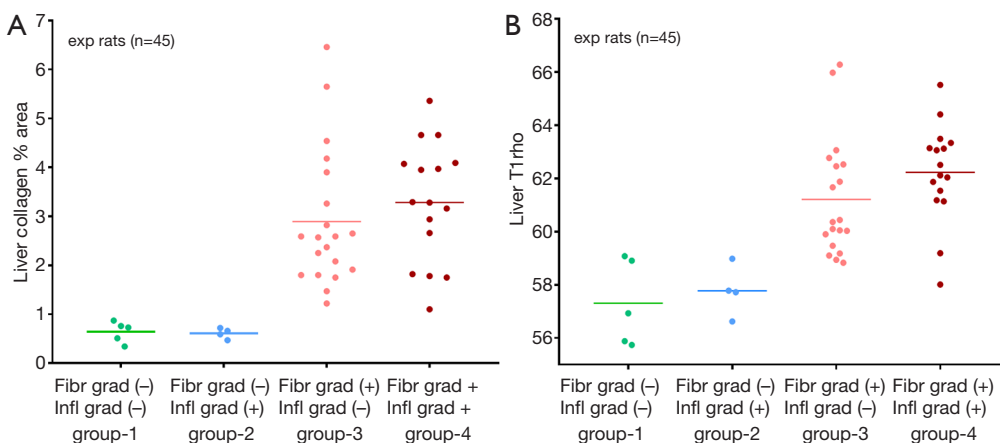


**Figure 6** In experimental rats, liver T1rho measure broadly mirrors liver collagen content. (A) Liver collagen area (measured in percentage area by histology). (B) Liver T1rho in milliseconds. Groups 1 and 2 rats did not develop positive fibrosis grading, group-2 rats differ from group 1 rats that they had positive inflammation grading (three rats of inflammation grade-1 and one rat of inflammation grade-2), the difference in liver T1rho between group 1 rats and group 2 rats are not substantial (the same as shown in Figure 3). Group-3 and group-4 rats had positive fibrosis grading and higher collagen content and longer T1rho measure than group 1 and 2 rats. Both group 2 rats and group 4 rats had positive inflammation grading, group 4 rats had much higher collagen content and much longer T1rho measure. Group 4 rats, which had positive inflammation grading, have slightly higher mean collagen content and have slightly longer mean liver T1rho than Group 3 rats which had only minimal inflammation (inflammation score=0).

with both higher liver collagen deposition (Figure 8C) and longer ‘apparent’ liver T1rho measures (Figure 8D).

For further clarification of liver fat and T1rho, four subgroups of experiment rats were selected where the

liver collagen had a narrow range within these subgroups, including six rats with liver collagen of 1.75–1.82% area, five rats with liver collagen of 2.57–2.66% area, five rats with liver collagen of 2.94–3.29% area, and five rats

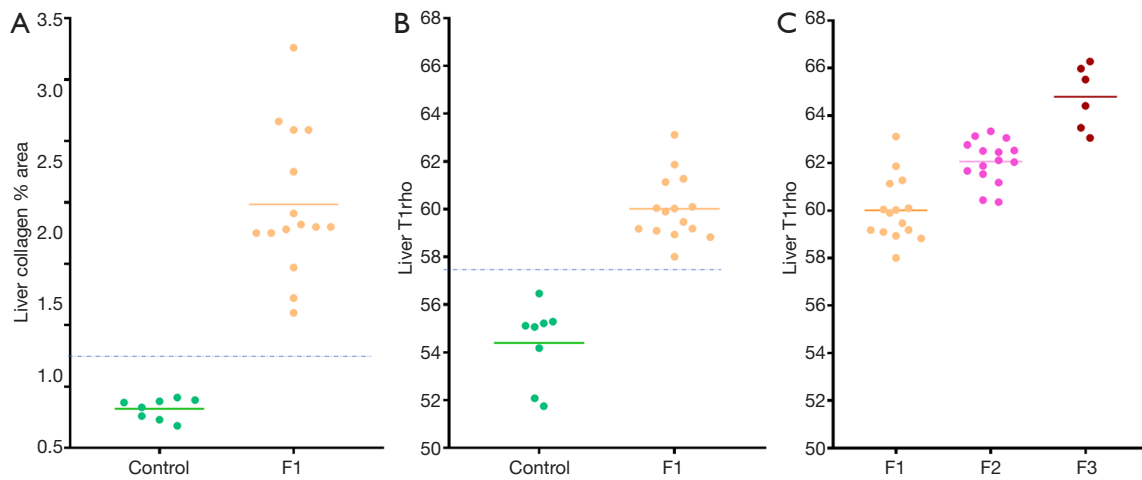


**Figure 7** T1rho can separate control rat livers (n=8) and stage-1 fibrosis rat livers (n=15) completely. (A) Liver collagen contents (measured in percentage area by histology) of control rats and stage-1 fibrosis rats forms two clusters which can be separated; (B) liver T1rho (in milliseconds) of control rats and stage-1 fibrosis rats; (C) higher histology fibrosis grading is associated with higher liver T1rho measure. F1, stage-1 fibrosis; F2, stage-2 fibrosis; F3, stage-3 fibrosis bar: mean.

with liver collagen of 3.9–4.09% area (Figure 9). All four subgroups showed a trend of negative correlation between liver fat and liver T1rho.

## Discussion

The clinical spectrum of NAFLD ranges from fatty liver with intracellular lipids exceeding 5% of the hepatic tissue, fatty liver with infiltration of inflammatory cells (referred to as NASH) and signs of liver injury (e.g., ballooning hepatocytes), and can progress to fibrosis and cirrhosis. The MCD model aims to mimic NAFLD in human (22,23). Methionine and choline deficiency rapidly induce steatohepatitis in rodents. Triglycerides and lipoperoxides accumulate, and while these changes are variable, levels usually become significantly increased compared to appropriate dietary controls after 2–5 days of MCD feeding. After 3 weeks of MCD feeding, steatohepatitis is well developed, and by 8–10 weeks pericellular and perisinusoidal fibrosis are present. After 10 weeks of dietary feeding, there is extensive macrovesicular steatosis in all zones except the periportal region, together with multiple foci of necroinflammation in the liver. The hepatic inflammatory infiltrate includes lymphocytes and neutrophils. Perivenular and pericellular fibrosis, the so-called chicken-wire fibrosis typically seen in human NASH, also readily develops (22,23). Leaving aside the issue that histology misses many aspects of *in vivo* process such as edema, the current study using

MCD model strongly suggest that collagen deposition alone can lead to liver T1rho elongation. T1rho is highly sensitive to liver collagen content. As shown in this study even the variation of liver collagen content in healthy control rats can be observed with a positive correlation. In the current study, 1% collagen increase contributed to approximately 1.4 ms T1rho relaxation time elongation.

We have previously reported that liver T1rho is positively associated with liver collagen deposition in the rat BDL model (1,3). In BDL model, increased intraluminal pressure is a mechanism of initiating entry of biliary epithelial cells into the replicative cycle. Stellate cells activated and transformed into myofibroblasts and thus fibrogenesis developed. On the other hand, inflammatory reactions associated with this model is mild, even at day-16 after BDL (24,25). The positive correlation between T1rho and fibrosis has also been reported by Hector *et al.* (26), where they reported T1rho values were significantly higher in the cortex of fibrotic *vs.* functional kidney allografts ( $111.8 \pm 17.2$  *vs.*  $99.0 \pm 11.0$  ms). Cortical T1rho significantly correlated with Masson's trichrome-stained fractions. Renal allograft fibrosis, associated with the deposition of collagen in the cortical interstitial space, is considered an important factor for allograft prognosis. In another study, Hector *et al.* (27) reported that spleen T1rho showed a significant correlation with portal pressure and clinically significant portal hypertension. It was suggested that the elevation in T1rho in the spleen with increased portal hypertension

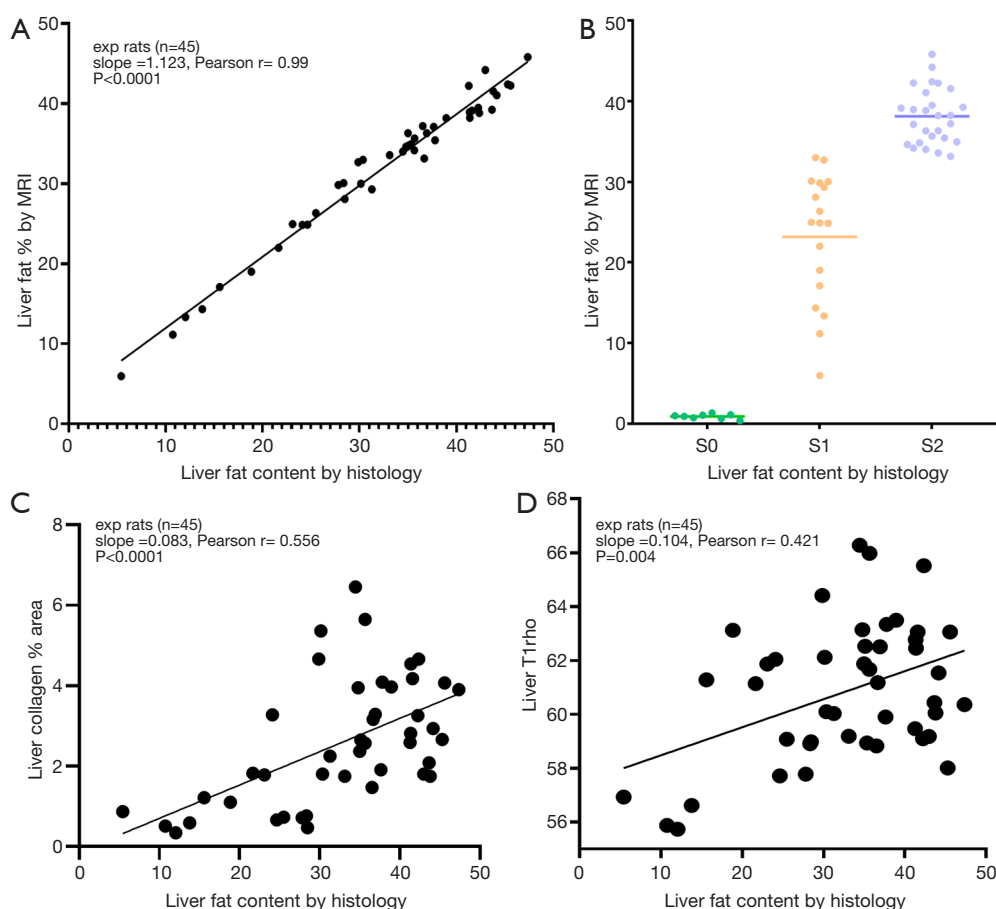


**Figure 8** Fat content' effect on liver collagen. (A) Correlation between fat content measured by MRI and by histology (measured in percentage area); (B) correlation between fat content measured by MRI and histology score (45 experimental rats); (C) higher liver fat content is associated with higher liver collagen content; (D) higher liver fat content is associated with 'apparent' longer T1rho measure (in milliseconds).

severity may reflect the deposition of collagen associate with fibrogenesis (27).

This study showed a weak trend that higher liver inflammation was associated longer liver T1rho measure, while rats with no or minimal inflammation could also have very high T1rho value (Figure 4B). While inflammation, particularly *in vivo* inflammation, can contribute to T1rho elevation to some degree (2), it is possible that the correlation between liver T1rho measure and liver inflammation in this study is more mediated via liver collagen content, as severe inflammation tends to induce more collagen deposition. On the other hand, with a CCl<sub>4</sub> intoxication rat model of live inflammation and fibrosis, Xie *et al.* (6) reported liver T1rho values mildly correlated with fibrosis stages ( $r=0.362$ ) and moderately correlated with grades of inflammation ( $r=0.568$ ). The T1rho values of rats

with the same inflammation grades showed no significant difference among different fibrosis stages. They concluded that inflammation grade was an independent variable associated with T1rho values, and inflammatory activity had a greater impact on liver T1rho values than fibrosis. Their results differ from the results of our studies. A few points should be considered. Firstly, CCl<sub>4</sub>-induced liver fibrosis is associated with a greater extent of inflammation, with greater extent of edema, infiltration of inflammation cells, degeneration, and necrosis of hepatocytes than BDL model and MCD model. It is accepted that the causes of liver T1rho elongation *in vivo* would be multi-factorial, and indeed inflammatory changes would contribute to liver T1rho elevation (2), but MCD diet model is a more clinically relevant animal model. Secondly, the fibrosis extent in the study of Xie *et al.* was not quantified as in this

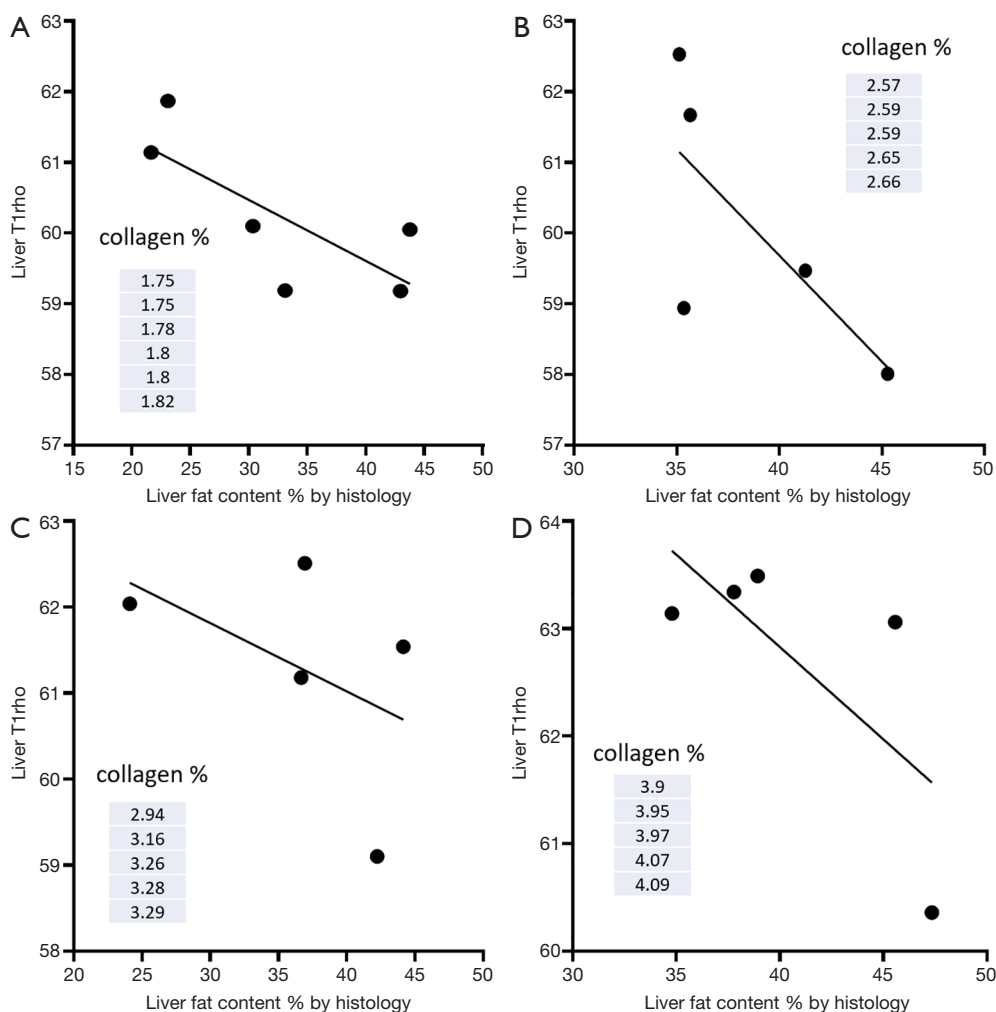


**Figure 9** Experimental rats show a trend of negative correlation between liver fat and liver T1rho (in milliseconds) when the liver collagen content is controlled. Subgroup of A, B, C, D each has 6, 5, 5, 5 rats, respectively. Collagen %: collagen area in percentage by histology.

study, instead they only offered subjective grading. Thirdly, it is less convincing that after withdrawal of CC4 for 3 or 4 weeks, liver T1rho values would have shortened to the levels substantially lower than the baseline measure (Figure 2 of Xie *et al.*'s article).

The same as previous reports (28), this study demonstrated the correlation between MRI-PDFP measure and histology measure of T1rho was robust. In a clinical observation, Xie *et al.* reported simple steatosis does not elongate liver T1rho (14). The current study shows liver fat actually shorten T1rho. For Figure 9, if liver fat had no effect on T1rho, a weak positive correlation would be expected, as from the fibrosis pathogenesis point of this MCD model, higher liver fat would be associated

higher extent of liver inflammation and then higher extent of collagen deposition in the liver. Higher liver fat was associated with higher extent of collagen deposition in the liver is shown in Figure 8C of this study. In this study, despite fat suppression technique is applied satisfactorily (Figure 1), Figure 9 shows all four subgroups had a trend of negative correlation between liver fat and liver T1rho. Thus, the relationship observed in Figure 8D might be due to that higher liver fat was associated with higher liver collagen, while the relation between collagen and T1rho was dominant. Liver fat contributes to T1rho decrease would partially explain our previous report on volunteer subjects that men tended to have shorter T1rho than women and older subjects had shorter liver T1rho than

younger subjects (29,30). It is known older age subjects are associated higher prevalent of liver steatosis, and liver steatosis is more prevalent in men than women up to the age of 60 years. Beyond menopause, the prevalence of fatty liver rises sharply in women and may exceed that observed in their male counterparts (31-33).

Both animal experiments and clinical studies have revealed that liver fibrosis, even early cirrhosis, is reversible, treatment with combined therapies on underline etiology and fibrosis simultaneously might expedite the regression of liver fibrosis and promote liver regeneration (34-37). Earlier stage liver fibrosis is more amenable to therapeutic intervention. Even when the underline etiology of liver fibrosis could not be eradicated, therapies on liver fibrosis might help restrict the disease progression to cirrhosis. Therefore, early detection of liver fibrosis and treatment monitoring is of paramount importance. T1rho MRI has the advantage of no additional hardware is needed, the imaging post-processing is straightforward, and also T1rho measurement can have very good scan-rescan reproducibly if a right T1rho acquisition method is applied (29,30). In addition to our pre-clinical study with BDL model suggesting that T1rho MRI alone allow differentiation of normal livers and stage-1 liver fibrosis livers (3), it is interesting that our current study with diet induced NASH/fibrosis once again demonstrated T1rho MRI alone allow differentiation of normal livers and stage-1 liver fibrosis livers (Figure 7). On other hand, while stage 1, 2, and 3 fibrotic livers had different mean T1rho values, the separation of these three groups by T1rho was not discreet. Our explanation is that increased liver T1rho primarily reflect increased collagen content, while staging of fibrosis is more subjective and also more reflect the structural distribution of fibrotic formations.

Compared with animal model results, till now the evidences from human studies suggest the clinical application may be more challenging which may be related to the wide range of physiological T1rho measures in healthy livers and also the narrow dynamic range of T1rho for diseased livers (10,11,13-19,30). Liver physiology has variations related to age and gender which in turn are affected by variations of iron/fat deposition and perfusion changes. Aging is associated with increased iron deposition and decreased blood perfusion with this phenomenon being more prominent among women after menopause (30,38-43). In addition to develop sequences to compensate or remove iron related T2\* effect and fat's effect during T1rho analysis, one apparent strategy for clinical study is to use age-

and gender-matched subjects as controls. Moreover, the combined application of hepatocyte specific contrast agents and T1rho may improve the diagnostic performance (5,16). Stief *et al.* (16) performed T1rho-weighted images before Gd-EOB-DTPA contrast agent administration. Gd-EOB-DTPA-enhanced MR images were acquired before and 20 min after injection of 0.1 ml/kg body weight of Gd-EOB-DTPA. 'Relative Enhancement' was calculated as  $(S_{20\text{min}} - S_{\text{unenanced}})/S_{\text{unenanced}}$  and 'Fibrosis Function Quotient' was calculated as 'T1rho/ Relative Enhancement'. Fibrosis Function Quotient improved diagnostic performance for cirrhotic noncirrhotic liver. In a study of rabbit model, Xie *et al.* (5) reported T1rho imaging during the hepatobiliary phase of Gd-EOB-DTPA allowed a total separation of normal livers and livers with NASH, such a differentiation was better than T1rho alone. In their study, the T1rho and Gd-EOB-DTPA enhanced T1rho for control rabbit livers was  $40.50 \pm 1.34$  and  $34.37 \pm 1.74$  ms respectively, while the T1rho and Gd-EOB-DTPA enhanced T1rho for rabbit livers with NASH was  $45.48 \pm 2.40$  and  $42.31 \pm 3.07$  ms (mean difference between control rabbits and NASH rabbits: 4.98 ms for native T1rho and 7.94 ms for enhanced T1rho).

Magnetic resonance elastography (MRE) is one of the most promising MR imaging techniques for liver fibrosis, which quantitatively assesses liver tissue stiffness by analysis of shear waves induced in the liver by low-frequency vibrations applied to the abdominal wall (44,45). However, MRE needs a specific external equipment, and remains challenging in the detection of early-stage liver fibrosis. Elastography methods require propagation of mechanical waves into the tissue of interest. Wave propagation may be limited in obese patients. High hepatic iron overload also leads to MRE exam non-diagnostic (46). It is likely that a multi-parametric approach will have even better accuracy for evaluating the spectrum of chronic liver disease (5,47-51). In their study with MCD rabbit model, Xie *et al.* (5) reported that a combination of T1rho at Gd-EOB-DTPA-enhanced hepatobiliary phase and IVIM (Intravoxel incoherent motion) derived perfusion fraction had a very high diagnostic value for NASH (AUC: 0.971). Recently Wang (48) proposed that liver vessel density can be measured by a diffusion weighted imaging derived surrogate biomarker [diffusion derived vessel density (DDVD)] which refers to the signal difference between images when the diffusion gradient is off (where blood vessels show high signal) and images when the diffusion gradient is on (where blood vessels show signal void). DDVD measure has the advantage of simplicity, and image data can be potentially

acquired by a single breath-hold. It has been shown that DDVD is correlated to the IVIM perfusion parameters perfusion fraction and  $D_{\text{fast}}$  (perfusion associated diffusion), and is a useful biomarker for the separation of livers with and without fibrosis, and livers with severe fibrosis tend to have even lower DDVD measurements than those with milder liver fibrosis (49). Moreover, the combination of DDVD and IVIM parameters improves the separation of fibrotic and nonfibrotic livers (49).

There are a few limitations of this study. The T1rho values for control rats in this study, ranging 51.7–56.47 ms ( $54.40 \pm 1.65$  ms) for control rat livers, were slightly higher than our former studies (1–3). This may be related to the T1rho sequence configuration as well as imperfect TSLs selected in this study. However, the CoV of healthy liver T1rho in this study (0.03) was similar or better than our previous studies [0.0399 in reference (3), 0.0452 in reference (1)]. On the other hand, T1rho measure can be relatively robust for the same sequence configuration (52,53). The reference standard used in this study was histology, which was not a perfect comparison with *in vivo* MRI measurement. Histology does not assess edema, vessel dilatation, etc which are measure by *in vivo* MRI. Our previous study using  $\text{CCl}_4$  intoxication suggests edema may slightly contribute to T1rho elevation (2). ‘Fibrosis process’ includes collagen deposition and inflammation, it can be considered that collagen deposition is a reaction to inflammation. Severe inflammation tends to induce more collagen deposition. To disentangle what is contributed by inflammation and what is contributed by collagen deposition can be difficult. Histological grading of ‘fibrosis’ is primarily based on the severity ‘collagen deposition’, while reflects less on inflammation components. In the meantime, the semi-quantitative inflammation scoring system used in this study may still lack sufficient details (21). Moreover, histology grading and scoring are associated with subjectivity and potential sampling bias.

In conclusion, this study with an MCD diet rat model suggests collagen deposition in the live strongly contributes to liver T1rho elongation, while fat deposition contributes to T1rho shortening. In a well-controlled experimental setting, T1rho measure alone allows separation of healthy livers and stage-1 liver fibrosis in the MCD model. Together with previous studies, this study further supports the potential of T1rho MRI for assessing early stage liver fibrosis. After removing the confounding factors such liver iron and fat contents, or in the combination of hepatocyte specific contrast agent, T1rho may be able to play important

roles in liver fibrosis management, both for early detection as well as longitudinal monitoring.

## Acknowledgments

The authors thank Dr. J. Chiel den Harder, Prof. Aart J. Nederveen, and Dr. Qinwei Zhang at Dept Radiology and Nuclear Medicine, Amsterdam University Medical Center, The Netherlands, for providing the T1rho sequence used in this study, and thank Yuan Hong, Zhejiang University, for supports in this study.

**Funding:** This study was supported by the National Nature Science Foundation of China (81701683 & 81771805), Hong Kong GRF grant (Project No. 14109218), Health Commission of Zhejiang Province (2020KY131), Zhejiang Provincial Natural Science Foundation of China (LQ15H180001 & LY17H180001) and Zhejiang Provincial Key Discipline of Traditional Chinese Medicine (2017-XK-A32).

## Footnote

**Conflicts of Interest:** All authors have completed the ICMJE uniform disclosure form (available at <http://dx.doi.org/10.21037/qims-20-651>). YXJW serves as an unpaid Editor-in-Chief of *Quantitative Imaging in Medicine and Surgery*. The other authors have no conflicts of interest to declare.

**Ethical Statement:** This study was approved by the local Animal Experimentation Ethics Committee (NO. 2017-217), and conducted in compliance with institutional guidelines for the care and use of animals of Zhejiang University School of Medicine and Nanjing University Medical School, China.

**Open Access Statement:** This is an Open Access article distributed in accordance with the Creative Commons Attribution-NonCommercial-NoDerivs 4.0 International License (CC BY-NC-ND 4.0), which permits the non-commercial replication and distribution of the article with the strict proviso that no changes or edits are made and the original work is properly cited (including links to both the formal publication through the relevant DOI and the license). See: <https://creativecommons.org/licenses/by-nc-nd/4.0/>.

## References

1. Wang YX, Yuan J, Chu ES, Go MY, Huang H, Ahuja AT,

- Sung JJ, Yu J. T1rho MR imaging is sensitive to evaluate liver fibrosis: an experimental study in a rat biliary duct ligation model. *Radiology* 2011;259:712-9.
2. Zhao F, Wang YX, Yuan J, Deng M, Wong HL, Chu ES, Go MY, Teng GJ, Ahuja AT, Yu J. MR T1ρ as an imaging biomarker for monitoring liver injury progression and regression: an experimental study in rats with carbon tetrachloride intoxication. *Eur Radiol* 2012;22:1709-16.
  3. Koon CM, Zhang X, Chen W, Chu ES, San Lau CB, Wang YX. Black blood T1rho MR imaging may diagnose early stage liver fibrosis: a proof-of-principle study with rat biliary duct ligation model. *Quant Imaging Med Surg* 2016;6:353-363.
  4. Hu G, Zhang X, Liang W, Zhong X, Chan Q, Lin X, Lin T, Li Y, Quan X. Assessment of liver fibrosis in rats by MRI with apparent diffusion coefficient and T1 relaxation time in the rotating frame. *J Magn Reson Imaging* 2016;43:1082-9.
  5. Xie Y, Zhang H, Jin C, Wang X, Wang X, Chen J, Xu Y. Gd-EOB-DTPA-enhanced T1ρ imaging vs diffusion metrics for assessment liver inflammation and early stage fibrosis of nonalcoholic steatohepatitis in rabbits. *Magn Reson Imaging* 2018;48:34-41.
  6. Xie S, Qi H, Li Q, Zhang K, Zhang L, Cheng Y, Shen W. Liver injury monitoring, fibrosis staging and inflammation grading using T1rho magnetic resonance imaging: an experimental study in rats with carbon tetrachloride intoxication. *BMC Gastroenterol* 2020;20:14.
  7. Deng M, Zhao F, Yuan J, Ahuja AT, Wang YX. Liver T1ρ MRI measurement in healthy human subjects at 3 T: a preliminary study with a two-dimensional fast-field echo sequence. *Br J Radiol* 2012;85:e590-5.
  8. Wang YX, Zhao F, Wong VWS, Yuan J, Kwong KM, Chen HLY. Liver MR T1rho measurement in liver cirrhosis patients: a preliminary study with a 2D fast field echo sequence at 3T. *Proc Intl Soc Mag Reson Med* 2012;20:1289. Available online: <https://cds.ismrm.org/protected/12MProceedings/files/1289.pdf>
  9. Allkemper T, Sagmeister F, Cicinnati V, Beckebaum S, Kooijman H, Kanthak C, Stehling C, Heindel W. Evaluation of fibrotic liver disease with whole-liver T1ρ MR imaging: a feasibility study at 1.5 T. *Radiology* 2014;271:408-15.
  10. Rauscher I, Eiber M, Ganter C, Martirosian P, Safi W, Umgelter A, Rummeny EJ, Holzapfel K. Evaluation of T1ρ as a potential MR biomarker for liver cirrhosis: comparison of healthy control subjects and patients with liver cirrhosis. *Eur J Radiol* 2014;83:900-4.
  11. Takayama Y, Nishie A, Asayama Y, Ushijima Y, Okamoto D, Fujita N, Morita K, Shirabe K, Kotoh K, Kubo Y, Okuaki T, Honda H. T1 ρ Relaxation of the liver: A potential biomarker of liver function. *J Magn Reson Imaging* 2015;42:188-95.
  12. Singh A, Reddy D, Haris M, Cai K, Rajender Reddy K, Hariharan H, Reddy R. T1ρ MRI of healthy and fibrotic human livers at 1.5 T. *J Transl Med* 2015;13:292.
  13. Okuaki T, Takayama Y, Nishie A, Ogino T, Obara M, Honda H, Miyati T, Van Caueren M. T1ρ mapping improvement using stretched-type adiabatic locking pulses for assessment of human liver function at 3T. *Magn Reson Imaging* 2017;40:17-23.
  14. Xie S, Li Q, Cheng Y, Zhang Y, Zhuo Z, Zhao G, Shen W. Impact of Liver Fibrosis and Fatty Liver on T1rho Measurements: A Prospective Study. *Korean J Radiol* 2017;18:898-905.
  15. Chen W, Chen X, Yang L, Wang G, Li J, Wang S, Chan Q, Xu D. Quantitative assessment of liver function with whole-liver T1rho mapping at 3.0T. *Magn Reson Imaging* 2018;46:75-80.
  16. Stief JD, Haase M, Lüdemann L, Theilig D, Schmelzle M, Hamm B, Denecke T, Geisel D. Combined morphological and functional liver MRI using spin-lattice relaxation in the rotating frame (T1ρ) in conjunction with Gadoteric Acid-enhanced MRI. *Sci Rep* 2019;9:2083.
  17. Sharafi A, Baboli R, Zibetti M, Shanbhogue K, Olsen S, Block T, Chandarana H, Regatte R. Volumetric multicomponent T1ρ relaxation mapping of the human liver under free breathing at 3T. *Magn Reson Med* 2020;83:2042-50.
  18. Sirlin CB. Science to practice: Can T1rho imaging be used to diagnose and assess the severity of hepatic fibrosis? *Radiology* 2011;259:619-20.
  19. Wang YXJ, Chen W, Deng M. How liver pathologies contribute to T1rho contrast require more careful studies. *Quant Imaging Med Surg* 2017;7:608-13.
  20. Duvvuri U, Goldberg AD, Kranz JK, Hoang L, Reddy R, Wehrli FW, Wand AJ, Englander SW, Leigh JS. Water magnetic relaxation dispersion in biological systems: the contribution of proton exchange and implications for the noninvasive detection of cartilage degradation. *Proc Natl Acad Sci U S A* 2001;98:12479-84.
  21. Nascimbeni F, Ballestri S, Machado MV, Mantovani A, Cortez-Pinto H, Targher G, Lonardo A. Clinical relevance of liver histopathology and different histological classifications of NASH in adults. *Expert Rev Gastroenterol Hepatol* 2018;12:351-67.

22. Larter CZ, Yeh MM. Animal models of NASH: getting both pathology and metabolic context right. *J Gastroenterol Hepatol* 2008;23:1635-48.
23. Schattenberg JM, Galle PR. Animal models of non-alcoholic steatohepatitis: of mice and man. *Dig Dis* 2010;28:247-54.
24. Aller MA, Lorente L, Alonso S, Arias J. A model of cholestasis in the rat, using a microsurgical technique. *Scand J Gastroenterol* 1993;28:10-4.
25. Slott PA, Liu M, Tavoloni N. Origin, pattern and mechanism of bile duct proliferation following biliary obstruction in the rat. *Gastroenterology* 1990;99:466-77.
26. Hectors SJ, Bane O, Kennedy P, El Salem F, Menon M, Segall M, Khaim R, Delaney V, Lewis S, Taouli B. T1rho mapping for assessment of renal allograft fibrosis. *J Magn Reson Imaging* 2019;50:1085-91.
27. Hectors SJ, Bane O, Stocker D, Carbonell G, Lewis S, Kennedy P, Schiano TD, Thung S, Fischman A, Taouli B. Splenic T1ρ as a noninvasive biomarker for portal hypertension. *J Magn Reson Imaging* 2020;52:787-794.
28. Middleton MS, Heba ER, Hooker CA, Bashir MR, Fowler KJ, Sandrasegaran K, Brunt EM, Kleiner DE, Doo E, Van Natta ML, Lavine JE, Neuschwander-Tetri BA, Sanyal A, Loomba R, Sirlin CB; NASH Clinical Research Network. Agreement Between Magnetic Resonance Imaging Proton Density Fat Fraction Measurements and Pathologist-Assigned Steatosis Grades of Liver Biopsies From Adults With Nonalcoholic Steatohepatitis. *Gastroenterology* 2017;153:753-61.
29. Wáng YXJ, Deng M, Lo GG, Liang D, Yuan J, Chen W. Breath-hold black-blood T1rho mapping improves liver T1rho quantification in healthy volunteers. *Acta Radiol* 2018;59:257-65.
30. Wáng YXJ, Deng M, Lin J, Kwok AWL, Liu EKW, Chen W. Age- and Gender-Associated Liver Physiological T1rho Dynamics Demonstrated with a Clinically Applicable Single-Breathhold Acquisition. *SLAS Technol* 2018;23:179-87.
31. Gan L, Chitturi S, Farrell GC. Mechanisms and Implications of Age-Related Changes in the Liver: Nonalcoholic Fatty Liver Disease in the Elderly. *Curr Gerontol Geriatr Res* 2011;2011:831536.
32. Williams CD, Stengel J, Asike MI, Torres DM, Shaw J, Contreras M, Landt CL, Harrison SA. Prevalence of nonalcoholic fatty liver disease and nonalcoholic steatohepatitis among a largely middle-aged population utilizing ultrasound and liver biopsy: a prospective study. *Gastroenterology* 2011;140:124-31.
33. Ulbrich EJ, Fischer MA, Manoliu A, Marcon M, Luechinger R, Nanz D, Reiner CS. Age- and Gender Dependent Liver Fat Content in a Healthy Normal BMI Population as Quantified by Fat-Water Separating DIXON MR Imaging. *PLoS One* 2015;10:e0141691.
34. Gentile I, Scotto R, Zappulo E, Buonomo AR, Pinchera B, Borgia G. Investigational direct-acting antivirals in hepatitis C treatment: the latest drugs in clinical development. *Expert Opin Investig Drugs*. 2016;25:557-72.
35. Wang P, Koyama Y, Liu X, Xu J, Ma HY, Liang S, Kim IH, Brenner DA, Kisseleva T. Promising Therapy Candidates for Liver Fibrosis. *Front Physiol* 2016;7:47.
36. D'Ambrosio R, Aghemo A, Rumi MG, Ronchi G, Donato MF, Paradis V, Colombo M, Bedossa P. A morphometric and immunohistochemical study to assess the benefit of a sustained virological response in hepatitis C virus patients with cirrhosis. *Hepatology* 2012;56:532-43.
37. Marcellin P, Gane E, Buti M, Afdhal N, Sievert W, Jacobson IM, Washington MK, Germanidis G, Flaherty JF, Aguilar Schall R, Bornstein JD, Kitrinis KM, Subramanian GM, McHutchison JG, Heathcote EJ. Regression of cirrhosis during treatment with tenofovir disoproxil fumarate for chronic hepatitis B: a 5-year open-label follow-up study. *Lancet* 2013;381:468-75.
38. Wynne HA, Cope L, Mutch E, Rawlins M, Woodhouse K, James OFW. The effect of age upon liver volume and apparent liver blood flow in healthy man. *Hepatology* 1989;9:297-301.
39. Zoli M, Magalotti D, Bianchi G, Gueli C, Orlandini C, Grimaldi M, Marchesini G. Total and functional hepatic blood flow decrease in parallel with ageing. *Age Ageing* 1999;28:29-33.
40. Weinfeld A, Lundin P, Lundvall O. Significance for the diagnosis of iron overload of histochemical and chemical iron in the liver of control subjects. *J Clin Pathol* 1968;21:35-40.
41. Chen L, Zhu Z, Peng X, Wang Y, Wang Y, Chen M, Qi Wang Q, Jin J. Hepatic Magnetic Resonance Imaging With T2\* Mapping of Ovariectomized Rats: Correlation Between Iron Overload and Postmenopausal Osteoporosis. *Eur Radiol* 2014;24:1715-24.
42. Huang H, Zheng CJ, Wang LF, Che-Nordin N, Wáng YXJ. Age and gender dependence of liver diffusion parameters and the evidence of intravoxel incoherent motion modelling of perfusion component is constrained by diffusion component. *BioRxiv*. doi: <https://doi.org/10.1101/2020.08.27.271080>
43. Schwenzer NF, Machann J, Haap MM, Martirosian P,

- Schraml C, Liebig G, Stefan N, Häring HU, Claussen CD, Fritsche A, Schick F. T2\* relaxometry in liver, pancreas, and spleen in a healthy cohort of one hundred twenty-nine subjects—correlation with age, gender, and serum ferritin. *Invest Radiol* 2008;43:854-60.
44. Kennedy P, Wagner M, Castéra L, Hong CW, Johnson CL, Sirlin CB, Taouli B. Quantitative Elastography Methods in Liver Disease: Current Evidence and Future Directions. *Radiology* 2018;286:738-763.
  45. Wang XP, Wang Y, Ma H, Wang H, Yang DW, Zhao XY, Jin EH, Yang ZH. Assessment of liver fibrosis with liver and spleen magnetic resonance elastography, serum markers in chronic liver disease. *Quant Imaging Med Surg* 2020;10:1208-22.
  46. Ghos HM, Kröner PT, Stancampiano FF, Bowman AW, Vishnu P, Heckman MG, Diehl NN, McLeod E, Nikpour N, Palmer WC. Hepatic iron overload identified by magnetic resonance imaging-based T2\* is a predictor of non-diagnostic elastography. *Quant Imaging Med Surg* 2019;9:921-7.
  47. Wang YX, Wang X, Wu P, Wang Y, Chen W, Chen H, Li J. Topics on quantitative liver magnetic resonance imaging. *Quant Imaging Med Surg* 2019;9:1840-90.
  48. Wang YX. Living tissue intravoxel incoherent motion (IVIM) diffusion MR analysis without b=0 image: an example for liver fibrosis evaluation. *Quant Imaging Med Surg* 2019;9:127-33.
  49. Xiao BH, Huang H, Wang LF, Qiu SW, Guo SW, Wang YX. Diffusion MRI Derived per Area Vessel Density as a Surrogate Biomarker for Detecting Viral Hepatitis B-Induced Liver Fibrosis: A Proof-of-Concept Study. *SLAS Technol* 2020;25:474-83.
  50. Li T, Che-Nordin N, Wang YX, Rong PF, Qiu SW, Zhang SW, Zhang P, Jiang YF, Chevallier O, Zhao F, Xiao XY, Wang W. Intravoxel incoherent motion derived liver perfusion/diffusion readouts can be reliable biomarker for the detection of viral hepatitis B induced liver fibrosis. *Quant Imaging Med Surg* 2019;9:371-85.
  51. Kim JW, Lee YS, Park YS, Kim BH, Lee SY, Yeon JE, Lee CH. Multiparametric MR Index for the Diagnosis of Non-Alcoholic Steatohepatitis in Patients with Non-Alcoholic Fatty Liver Disease. *Sci Rep* 2020;10:2671.
  52. Zhao F, Deng M, Yuan J, Teng GJ, Ahuja AT, Wang YX. Experimental evaluation of accelerated T1rho relaxation quantification in human liver using limited spin-lock times. *Korean J Radiol* 2012;13:736-42.
  53. Yuan J, Zhao F, Griffith JF, Chan Q, Wang YX. Optimized efficient liver T(1p) mapping using limited spin lock times. *Phys Med Biol* 2012;57:1631-40.

**Cite this article as:** Zhao F, Zhou N, Wang JL, Zhou H, Zou LQ, Zhong WX, He J, Zheng CJ, Yan SX, Wang YXJ. Collagen deposition in the liver is strongly and positively associated with T1rho elongation while fat deposition is associated with T1rho shortening: an experimental study of methionine and choline-deficient (MCD) diet rat model. *Quant Imaging Med Surg* 2020;10(12):2307-2321. doi: 10.21037/qims-20-651